Journal of Digital Imaging (2023) 36:114–123
https://doi.org/10.1007/s10278-022-00698-5

ORIGINAL PAPER

Deep Learning for Detection of Intracranial Aneurysms from Computed Tomography Angiography Images

Xiujuan Liu[1] · Jun Mao[1] · Ning Sun[2] · Xiangrong Yu[1] · Lei Chai[2] · Ye Tian[1] · Jianming Wang[1] · Jianchao Liang[1] · Haiquan Tao[3] · Lihua Yuan[4] · Jiaming Lu[4] · Yang Wang[4] · Bing Zhang[4] · Kaihua Wu[3] · Yiding Wang[5] · Mengjiao Chen[5] · Zhishun Wang[6] · Ligong Lu[1]

Received: 26 September 2021 / Revised: 31 July 2022 / Accepted: 23 August 2022 / Published online: 9 September 2022

Abstract

The accuracy of computed tomography angiography (CTA) image interpretation depends on the radiologist. This study aims to develop a new method for automatically detecting intracranial aneurysms from CTA images using deep learning, based on a convolutional neural network (CNN) implemented on the DeepMedic platform. Ninety CTA scans of patients with intracranial aneurysms are collected and divided into two datasets: training (80 subjects) and test (10 subjects) datasets. Subsequently, a deep learning architecture with a three-dimensional (3D) CNN model is implemented on the DeepMedic platform for the automatic segmentation and detection of intracranial aneurysms from the CTA images. The samples in the training dataset are used to train the CNN model, and those in the test dataset are used to assess the performance of the established system. Sensitivity, positive predictive value (PPV), and false positives are evaluated. The overall sensitivity and PPV of this system for detecting intracranial aneurysms from CTA images are 92.3% and 100%, respectively, and the segmentation sensitivity is 92.3%. The performance of the system in the detection of intracranial aneurysms is closely related to their size. The detection sensitivity for small intracranial aneurysms (≤ 3 mm) is 66.7%, whereas the sensitivity of detection for large (> 10 mm) and medium-sized (3–10 mm) intracranial aneurysms is 100%. The deep learning architecture with a 3D CNN model on the DeepMedic platform can reliably segment and detect intracranial aneurysms from CTA images with high sensitivity.

Keywords Deep learning · Computed tomography angiography · Intracranial aneurysm · Convolutional neural networks · Computer-aided diagnosis

Introduction

An intracranial aneurysm is a protrusion of a cerebral artery due to a local congenital defect or injury to the cerebral artery wall. It tends to occur in middle-aged and elderly people between the ages of 40 and 60 years [1]. A cerebral arterial circle near the skull base, called the circle of Willis, is a crucial circulatory anastomosis that supplies blood to the brain and surrounding structures. The most common sites of intracranial aneurysms are the bifurcation of the circle of Willis and its main branches [2]. Intracranial aneurysms are the leading cause of spontaneous subarachnoid hemorrhage,

Xiujuan Liu and Jun Mao contributed equally and are joint co-first authors.

✉ Zhishun Wang
zw2105@cumc.columbia.edu

✉ Ligong Lu
learninzh@163.com

1 Department of Radiology, Zhuhai People's Hospital (Zhuhai Hospital Affiliated With Jinan University), Kangning Road, Xiangzhou District, Zhuhai, Guangdong 519000, China

2 Engineering Research Center of Wideband Wireless Communication Technology, Ministry of Education, Nanjing University of Posts and Telecommunications, Jiangsu, Nanjing 210000, China

3 Department of Neurosurgery, Zhuhai People's Hospital (Zhuhai Hospital Affiliated With Jinan University) Zhuhai, Guangdong 519000, China

4 Department of Radiology, The Affiliated Drum Tower Hospital, Nanjing University Medical School, Nanjing 210000, Jiangsu, China

5 CT Room, The First Affiliated Hospital of Harbin Medical University, Harbin, Heilongjiang 150001, China

6 Department of Psychiatry, Vagelos College of Physicians and Surgeons, Columbia University, NY 10032, USA

accounting for approximately 70–85% of cases [3, 4]. Cerebrovascular accidents rank third, after cerebral thrombosis and hypertensive intracerebral hemorrhage, and the incidence of ruptured intracranial aneurysms is 4–16 per 100,000 people per year [5]. Moreover, the mortality and disability rates are approximately 30% and 70%, respectively, after the first and second hemorrhages. In addition, untreated intracranial aneurysms have a 5-year mortality rate of 75%. Therefore, the detection, diagnosis, prevention, and treatment of intracranial aneurysms are active fields of medical research.

Digital subtraction angiography (DSA), CTA, and magnetic resonance angiography (MRA) are commonly used to examine intracranial aneurysms. DSA has been regarded as the gold standard for the diagnosis of intracranial aneurysms; however, it has several disadvantages, such as high cost, long procedure time, high invasiveness, high radiation dose, and high technical requirements for operators [6]. CTA and MRA are widely used as noninvasive vascular examination methods in clinical practice [7]. Compared with CTA, MRA is rarely used as a diagnostic method for intracranial aneurysms because of its longer examination time, lower vascular spatial resolution, and greater incidence of missed diagnosis and misdiagnosis of small intracranial aneurysms [8]. CTA is the preferred method for the diagnosis of intracranial aneurysms because of its simplicity, fast examination speed, low cost, high spatial resolution, and the ability to freely rotate the image. However, all three diagnosis methods are highly dependent on well-trained radiologists for the interpretation of the images for the ultimate diagnostic reports. The accuracy and time taken for interpretation depend on the expertise of the radiologists; thus, inconsistent diagnostic outcomes are often produced. In addition, with the increasing workload of radiology departments providing various imaging diagnostic services, fatigue caused by overwork may cause radiologists to neglect or misinterpret potentially relevant findings. Therefore, a reliable artificial intelligence (AI) system must be developed to aid radiologists in interpreting CTA images for quick and accurate diagnosis of intracranial aneurysms. The development of AI systems will have important clinical value in shortening the diagnosis time and reducing the missed diagnosis or misdiagnosis caused by different professional levels or work fatigue of radiologists.

Two types of AI systems have been proposed to aid in diagnosing intracranial aneurysms: conventional computer-aided diagnosis methods based on machine learning algorithms with manual features [8–10], and more recently, diagnosis methods based on deep learning algorithms [11, 12]. Conventional computer-aided diagnosis methods based on machine learning algorithms have some limitations as they typically require input by experts of clearly recognizable features. In contrast, deep learning is an emerging subset of machine learning techniques that imitates the cognitive mechanisms of the human brain and can automatically learn feature representations in a general manner [13]. The vast majority of deep learning models are implemented in the form of large-scale deep neural networks, among which deep convolutional neural networks (CNNs) have achieved considerable success in the field of image and video analyses. Compared to traditional models based on shallow learning, CNN has fewer manual interventions during the training process and adjusts the parameters in the network using the back-propagation algorithm [14–16]. When the training dataset is sufficiently large, the image analysis performance achieved by the CNN model is far superior to that of traditional methods.

Recently, deep learning methods have been applied for the automated detection of intracranial aneurysms from MRA images [11, 12]. The deep learning algorithms were based on CNN models and were implemented on the open platform DeepMedic (https://github.com/deepmedic). Considering the disadvantages of MRA images, automatic detection of intracranial aneurysms from CTA images based on deep learning models has also been reported [17–19]. Although these reported methods have shown good application potential compared to MRA-based deep learning methods, they still have limitations, such as poor performance in the diagnosis of small intracranial aneurysms (intracranial aneurysms smaller than 3 mm were simply ignored) [18], or low detection sensitivity (approximately 50%) [19]).

Therefore, to further improve the performance of methods based on deep learning, a novel method based on three-dimensional (3D) CNN models implemented on the DeepMedic platform was developed for the automated segmentation and detection of intracranial aneurysms from CTA images. The new system based on 3D CNN models automatically detects intracranial aneurysms from CTA images, particularly those with small intracranial aneurysms (< 3 mm), thus thereby proving its applicability and potential for clinical use.

Methods

Sample Collection and Dataset

From 2016 to 2019, we retrospectively collected 90 CTA scans of patients with intracranial aneurysms at two centers in China: the Radiology Department of Zhuhai People's Hospital and the Radiology Department of the First Affiliated Hospital of Harbin Medical University. The 90 CTA images were acquired from patients who had undergone both CTA and DSA examinations or surgical treatment and in which the DSA examination or surgical treatment confirmed intracranial aneurysms. The demographic information of these patients, which included their basic

medical record information, surgery, and DSA report information, was collected. The selected 90 cases were arranged in alphabetical order according to the names of the patients. The first 80 randomized cases were used as the training dataset, and the last 10 were used as the test dataset. After grouping, de-identification procedures were performed to delete the protected health information of the patients, including name, date of birth, medical record number, and examination date. The inclusion criteria for these cases were as follows. (1) a radiology CTA report of a suspected untreated intracranial aneurysm; (2) the same patient underwent a DSA examination or a clipping operation after the CTA examination, and the DSA or intraoperative results confirmed an intracranial aneurysm. The exclusion criteria were as follows: (1) patients who had already undergone aneurysm embolization or clipping, including patients with multiple aneurysms, of which one aneurysm had been embolized or clipped; (2) patients who only had CTA of the head for suspected aneurysms but did not undergo DSA angiography or surgery; (3) poor image quality and motion artifacts; (4) patients with neoplastic lesions of the nervous system; (5) outpatients with incomplete clinical data; and (6) patients who underwent magnetic resonance imaging time-of-flight angiography (MRI-TOF) examination but did not undergo the CTA examination. This retrospective study was approved by the Ethics Committee of Zhuhai People's Hospital and the First Affiliated Hospital of Harbin Medical University. Informed consent was obtained from all participants.

A 256-slice CT scanner (Brilliance ICT; Philips Healthcare, Best, The Netherlands) was used for CTA. During the CTA examination, the patient's head was fixed in a neutral position to prevent motion artifacts, and the scan range covered from the cranial base to the cranial vault. The parameters for CTA acquisition were: 120 kV, 250 mAs, 64×0.625 mm detector collimation, 0.5 s gantry rotation time, 0.985 pitch, 0.9-mm section thickness, 0.45 mm increment, 220 mm FOV, 512×512 matrix, and standard brain reconstruction method (Philips Medical Systems). The CTA protocol was performed after 70 ml of a nonionic contrast medium (iopromide, 370 mg iodine/ml, Ultravist, Bayer Schering, Berlin, Germany) was injected into the antecubital vein with an automatic electric syringe at a flow rate of 5 ml/s, followed by 30 ml of normal saline.

Preprocessing of CTA Images

The preprocessing steps for the CTA images were as follows. (1) The CTA image data were converted from DICOM format to NIfTI format using ITK-SNAP software (version 3.6.0; www.itksnap.org). (2) Intracranial aneurysms were manually segmented using ITK-SNAP software and stored as NIfTI files. (3) The range of intracranial arteries on the *X*-, *Y*-, and *Z*-axes was discovered and recorded using the ITK-SNAP software, and the upper and lower boundaries and front and back boundaries of the intracranial artery were manually determined. This procedure was conducted to maintain the intracranial arteries within the test range as much as possible and to minimize the interference of the skull. (4) Based on the range determined in step 3, a MATLAB script was used to remove parts of the images beyond the range and evenly crop the original images to a size of $400 \times 400 \times 227$. (5) The cropped images were normalized using MATLAB.

DeepMedic Platform and Evaluation

DeepMedic is an open software platform for deep learning algorithms based on a 3D CNN for brain lesion segmentation. The implementation of the DeepMedic platform has shown good prospects in the segmentation of traumatic brain lesions, brain tumors, and ischemic stroke. In this study, a 3D CNN architecture (Fig. 1) was implemented using the DeepMedic 6.1, platform (https://biomedia.doc.ic.ac.uk/software/deepmedic) for the automatic segmentation and detection of intracranial aneurysms from CTA images.

A multi-scale and dual-channel 3D-CNN model was implemented using the DeepMedic platform, which consisted of two pathways: normal resolution and low resolution. The input of the low-resolution pathway was a subsampled version of that of the normal-resolution pathway (Fig. 1). This dual-channel architecture extracts considerable detailed information from the normal-resolution pathway and maintains a large range of overall information in the low-resolution pathway to ensure accuracy in the segmentation information and correct the location information. The parameters were set as proposed by Kamnitsas et al. [20]; the initial learning rate was 10^{-3} and was gradually reduced. For the optimization, the Nesterov momentum was set to 0.6. The CNN model was trained with dropout and regularization of $L1 = 10^{-6}$ and $L2 = 10^{-4}$, respectively. To accelerate the convergence, rectified linear unit activation functions and batch normalization were used in the DeepMedic platform, and a satisfactory effect was achieved. Subsequently, the proposed DeepMedic hybrid sampling scheme was used, wherein the image segments larger than the receptive field of the neural network were considered the input of the network, which effectively solved the problem of uneven distribution of voxel classes in the image segmentation.

On the DeepMedic platform, the automatic segmentation and detection processes of intracranial aneurysms from CTA images were divided into two stages: training and testing. In the training stage, 80 labeled preprocessed CTA images were used to train the 3D CNN segmentation system. In the

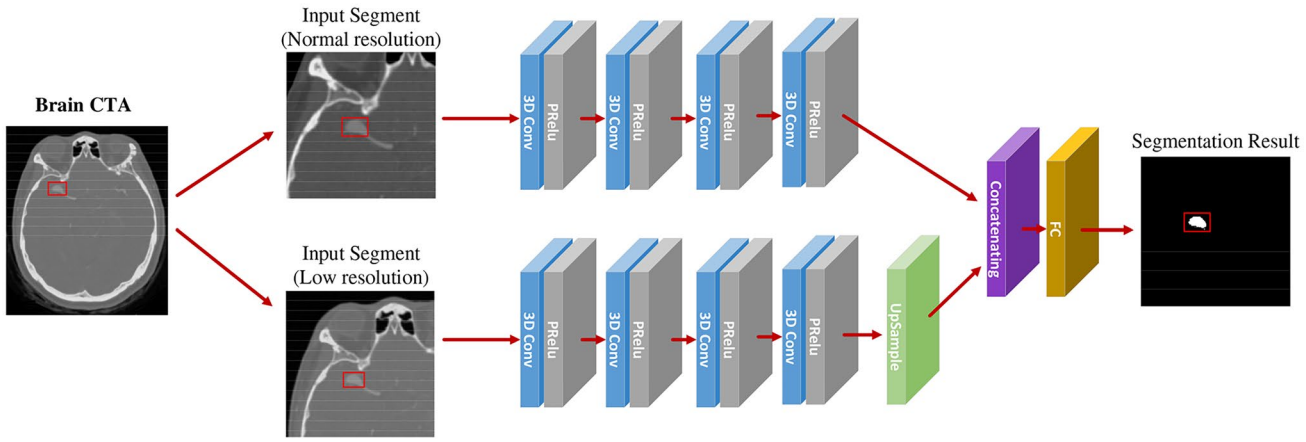

Fig. 1 Flowchart of the CNN based on the DeepMedic model

testing stage, 10 unlabeled preprocessed CTA images were used to verify the ability of the CNN system to segment intracranial aneurysms. After testing, the system outputted two types of images: a binary segmentation image, where 1 represented the regions containing an intracranial aneurysm, and 0 represented the regions where an aneurysm was not detected; and a continuous likelihood segmentation image representing a probability or confidence value between 0 and 1, which indicated a confidence degree within each area at which the likelihood of an intracranial aneurysm was evaluated. To validate the performance of the 3D CNN system in the automated segmentation of intracranial aneurysms from CTA images, the segmentation outcomes generated by the 3D CNN system and those manually labeled by a well-trained radiologist were compared.

Size and Location

To investigate the effects of intracranial aneurysm size and location on the detection rate, the intracranial aneurysm size was classified into three grades based on the maximum diameter: large (>10 mm), medium ($3<D\leq 10$ mm), and small (≤ 3 mm). Additionally, intracranial aneurysms were categorized into four locations: internal carotid artery (ICA); anterior circulation, including the anterior communicating artery (AcoA) and anterior cerebral artery (ACA); middle cerebral artery (MCA); and posterior circulation, including the vertebral artery (VA), basilar artery (BA), posterior cerebral artery (PCA), and posterior communicating arteries (PcoA).

Statistical Analysis

Using DSA or intraoperative diagnosis as a reference, the performance of the proposed deep-learning intracranial aneurysm segmentation system implemented on the DeepMedic platform was validated. The maximum and mean diameters of intracranial aneurysms were recorded as mean ± standard deviation (SD). The overall sensitivity of segmentation and detection and the positive predictive value (PPV) of detection were calculated for each intracranial aneurysm. Furthermore, the sensitivity and PPV of intracranial aneurysms were calculated based on their size and location. It was determined whether a false positive finding occurred in each output case; subsequently, the size, shape, confidence value (segmentation probability), and corresponding anatomical structure of the false positive findings were analyzed.

Results

General Information on the Training and Test Datasets

In the training dataset composed of 80 cases, 52 patients were female (65%), and 28 patients were male. The ages of the patients ranged from 31 to 84 years, with an average age of 60 years. Based on the gold standard of DSA or intraoperative findings, 98 untreated intracranial aneurysms were identified in 80 subjects, among which 68 had single intracranial aneurysms, seven had two aneurysms, four had three aneurysms, and one had four aneurysms. According to the results of DSA and intraoperative measurements, the maximum diameter of intracranial aneurysms ranged from 1.5 to 28.0 mm, and the average diameter was 7.1 ± 3.2 mm. As presented in Table 1, four aneurysms were < 3 mm, 74 aneurysms ranged in size from 3 to 10 mm, and 20 aneurysms were > 10 mm. The numbers of aneurysms located in the ICA, anterior circulation, MCA, and posterior circulation were 14, 22, 38, and 24, respectively (Table 2).

Table 1 The size of intracranial aneurysms in the training dataset and test dataset

Size	Number		Percentage (%)	
	Training	**Testing**	**Training**	**Testing**
< 3 mm	4	3 (1 false negative)	4	23
3–10 mm	74	7	76	54
> 10 mm	20	3	20	23
Total	98	13	100	100

In the test dataset of 10 cases, seven were female, and three were male. The age of the patients ranged from 53 to 78 years, and the average age was 64.3 years. Based on the gold standard, 13 untreated intracranial aneurysms were found in the 10 subjects, of which seven had single intracranial aneurysms, and three had two aneurysms. Three aneurysms had diameters < 3 mm, seven aneurysms had diameters ranging from 3 to 10 mm, and three aneurysms had diameters > 10 mm in the test dataset (Table 1). The maximum diameter range of intracranial aneurysms was 2.8 to 24.0 mm, and the mean diameter was 7.9 ± 3.6 mm. In addition, two, three, three, and five aneurysms were ICA, anterior circulation, MCA, and posterior circulation aneurysms, respectively.

Performance of the 3D CNN System in the Detection of Intracranial Aneurysms

For each intracranial aneurysm, the overall sensitivity and PPV of the 3D CNN segmentation system implemented through the DeepMedic platform were 92.3% and 100%, respectively. According to the size of each intracranial aneurysm, the sensitivity of the system to detect large (> 10 mm), medium (3–10 mm), and small (< 3 mm) intracranial aneurysms was 100, 100, and 66.7%, respectively, and the PPVs of the system for detecting each size of intracranial aneurysms were all 100% (Table 3). Considering the aneurysm locations, the sensitivity of the system to detect aneurysms in the ICA, anterior circulation, MCA, and posterior circulation was 100, 100, 100, and 80%, respectively (Table 4). The PPV values of the system to determine the size or location of intracranial aneurysms were all 100% (Tables 3 and 4).

Table 2 The location of intracranial aneurysms in the training dataset and test dataset

Location	Number		Percentage (%)	
	Training	**Testing**	**Training**	**Testing**
ICA	14	2	14	10
Anterior circulation aneurysm (ACA and AcoA)	22	3	22	24
MCA	38	3	39	26
Posterior circulation aneurysm (VA/BA/PCA/PcoA)	24	5 (1 false negative)	25	40
Total	98	13	100	100

ICA internal carotid artery, *ACA* anterior cerebral artery, *AcoA* anterior communicating artery, *MCA* middle cerebral artery, *VA* vertebral artery, *BA* basilar artery, *PCA* posterior cerebral artery, *PcoA* posterior communicating arteries

Table 3 Based on the size of the aneurysm, the detection capability of the Deepmedic framework

Size (mm)	DeepMedic framework	
	Sensitivity (%)	**PPV**
> 10	100	100
3–10	100	100
< 3	66.7	100

Performance of the 3D CNN System in the Segmentation of Intracranial Aneurysms

Of the 13 intracranial aneurysms in the test dataset, 12 were correctly segmented; thus, the overall segmentation sensitivity was 92.3%. Only one intracranial aneurysm was not segmented and showed one voxel at the location of the intracranial aneurysm. Among the 12 correctly segmented intracranial aneurysms, six aneurysms were completely consistent with the ground truth shape, with a mean confidence value of one in four intracranial aneurysms and 0.9999 in two intracranial aneurysms. The other six aneurysms were slightly smaller than the ground truth shape, with a mean confidence value of ≥ 0.95 in four intracranial aneurysms and 0.85–0.9 in two intracranial aneurysms. Using the actual shape of the aneurysm in the preprocessed CTA image as the reference standard, the shape auto-segmented by the 3D CNN segmentation system was compared with the shape manually segmented by a well-trained radiologist. The

Table 4 Based on the location of the aneurysm, the detection capability of the Deepmedic framework

Location	Deepmedic framework	
	Sensitivity (%)	**PPV**
ICA	100	100
Anterior circulation aneurysm	100	100
MCA	100	100
Posterior circulation aneurysm	80	100

ICA internal carotid artery, *MCA* middle cerebral artery

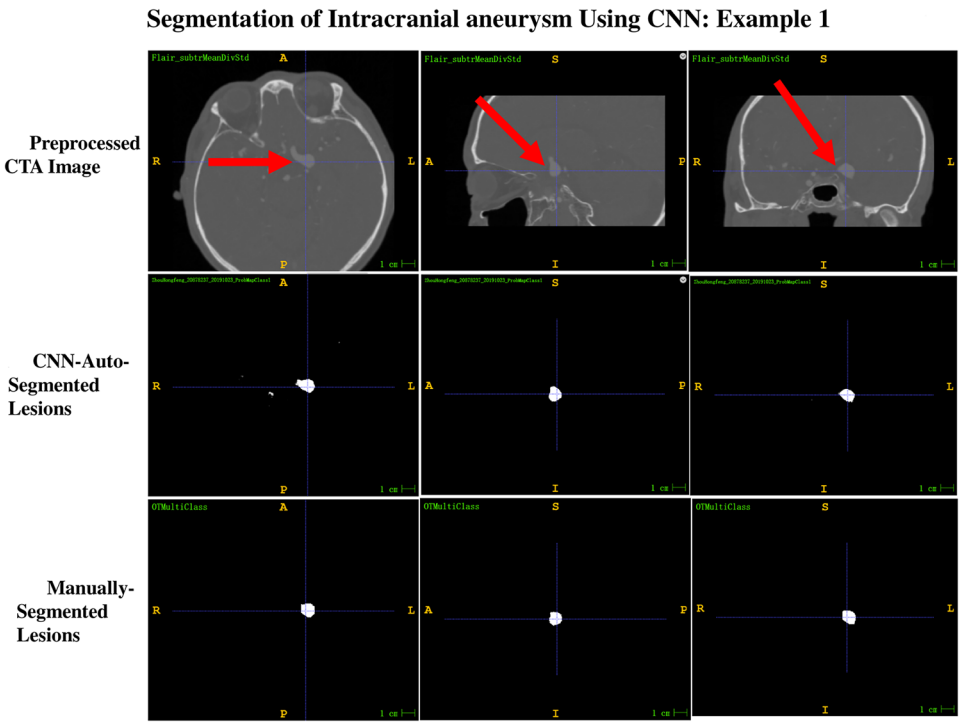

Fig. 2 Example 1 of the comparison between the shape auto-segmented by the 3D CNN segmentation system and that manually segmented by a well-trained radiologist, with ground truth as reference. The segmentation result of CNN-auto-segmented lesions is better than that of manually segmented lesions and is consistent with the ground truth shape of the preprocessed CTA images. The confidence value displayed by CNN-auto-segmented lesions was 1

evaluation revealed that 33.3% of aneurysms auto-segmented by the 3D CNN system were better than those with the manually segmented shape (Fig. 2), 16.7% were consistent with those with the manually segmented shape (Fig. 3), and 50% were slightly worse than those with the manually segmented shape (Fig. 4).

Analysis of False-Positive Findings

In each of the 10 output cases, some false-positive findings (also called false alarms) were observed. By comparing the output binary segmentation and output continuous likelihood segmentation images with the preprocessed CTA and

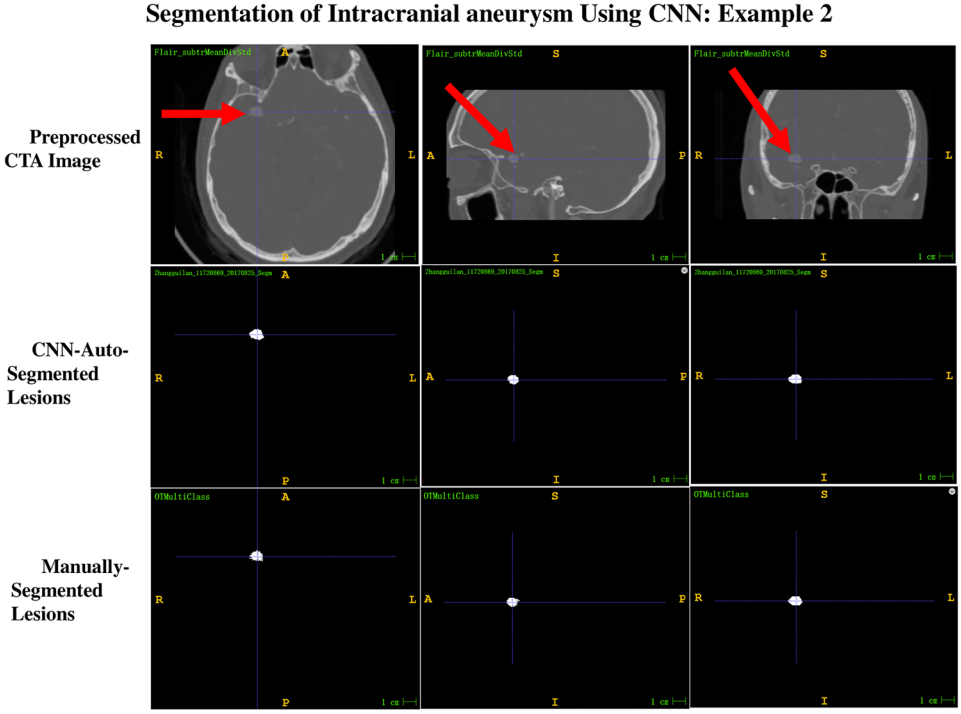

Fig. 3 Example 2 of the comparison between the shape auto-segmented by the 3D CNN segmentation system and that manually segmented by a well-trained radiologist, with ground truth as reference. The segmentation result of CNN-auto-segmented lesions is equivalent to that of manually segmented lesions and is consistent with the ground truth shape of the preprocessed CTA images. The confidence value exhibited by the CNN-auto-segmented lesions is 0.9999

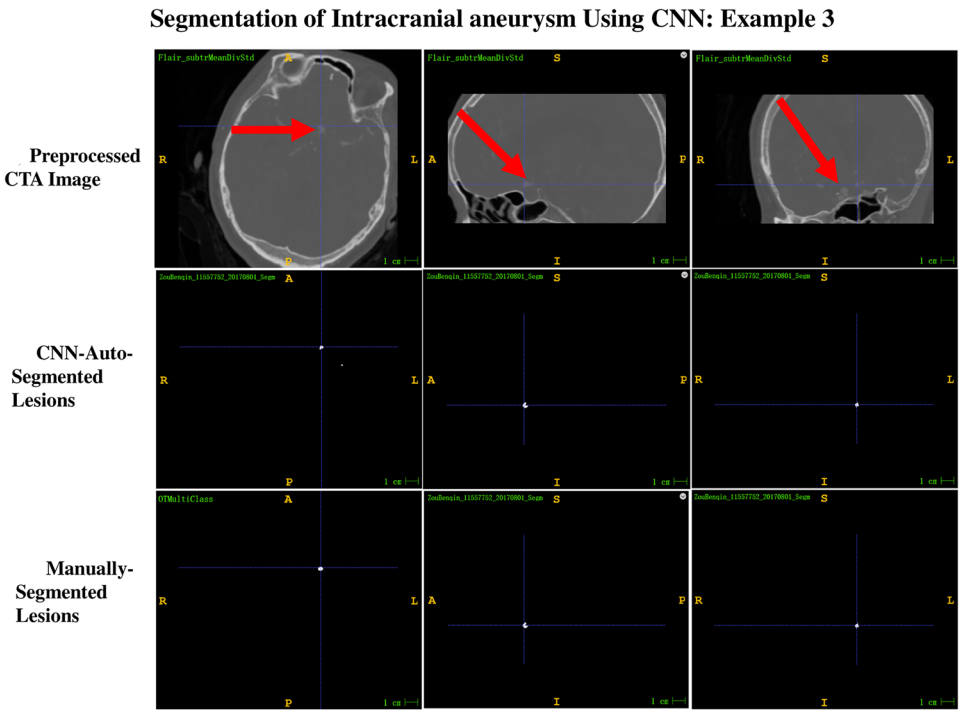

Fig. 4 Example 3 of the comparison between the shape auto-segmented by the 3D CNN segmentation system and that manually segmented by a well-trained radiologist, with ground truth as reference. The segmentation result of CNN-auto-segmented lesions is slightly worse than that of manually segmented lesions and is slightly smaller than the ground truth shape of the preprocessed CTA images. The confidence value exhibited by the CNN-auto-segmented lesions is 0.9957

manually segmented images, the size, shape, confidence values, and corresponding anatomical structure of the false-positive findings were recorded. The results are summarized as follows (Supplementary Table 1). In terms of size, 94.9% of false alarms were very small clusters with less than five voxels, wherein the vast majority had 1–2 voxels, and only 17 clusters had five or more voxels. Generally, a typical intracranial aneurysm has a cluster of more than 150 voxels; therefore, clusters with less than five voxels may simply represent noise. However, 16 clusters with more than five voxels were additionally investigated. Of these, five clusters were nonvascular, with most confidence values lower than 0.8, including one cluster representing dorsal sellar bone, one cluster representing pineal calcification, and three clusters representing calcified choroid plexuses in the lateral ventricle triangle. The remaining 11 clusters were 5–17 voxels in size, with confidence values all greater than 0.8 (some greater than 0.9). Among these, 10 represented cerebral artery regions with shape changes, and only one cluster represented a widened tentorial foot of the cerebellum (Fig. 5).

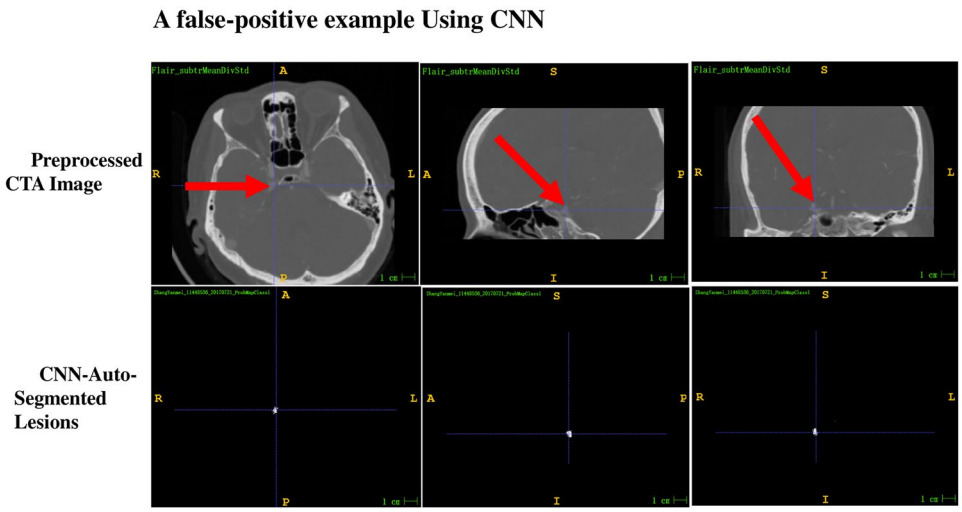

Fig. 5 Example of a false-positive finding using the 3D CNN segmentation system. Compared with the preprocessed CTA image (red arrow), the lesion is widened and enhances the right tentorial foot of the cerebellum. The confidence value is 0.8719

Discussion

Deep learning is an emerging branch of machine learning and has attracted increasing attention in the medical imaging field in recent years. CNN is one of the most commonly used deep learning architectures, and CNN-based methods have been proven to be more efficient than traditional feature extraction methods [13]. CNN models have been widely used in imaging applications, such as classification, segmentation, and object detection, and have shown satisfactory performance [12, 21–27]. The DeepMedic platform, which can be used to implement 3D CNN architectures, exhibits excellent performance in lesion segmentation of traumatic brain injury, brain tumor, and ischemic stroke [20, 28] and won the ischemic stroke lesion segmentation (ISLES) competition in 2015. Sichtermann et al. used the DeepMedic platform to detect intracranial aneurysms from 3D time-of-flight MRA (3DTOF-MRA) images [29]. However, owing to the technical limitations of MRA, CTA has been the preferred choice for the diagnosis of intracranial aneurysms. Therefore, in this study, DeepMedic was used for the first time to implement a 3D CNN architecture to automatically detect and segment intracranial aneurysms from CTA images, thereby achieving robust performance.

Our study demonstrated the considerable potential of a 3D CNN system based on DeepMedic for the reliable detection of intracranial aneurysms from CTA images. The overall sensitivity and PPV of this system were 92.3% and 100%, respectively, which are higher than those previously reported by Sichtermann et al. [29]. In the study by Sichtermann et al., DeepMedic was used to detect intracranial aneurysms from MRA images. Four different models were set up during the preprocessing stage according to skull processing strategies: one model did not remove the skull, whereas the other three models used different methods to remove it. Furthermore, four minimum false alarm thresholds of 0, 5, 6, and 7 mm^3 were set during the post-processing stage to reduce the number of false positives. In all the models, the highest sensitivity and PPV achieved by their systems were 90% and 57%, respectively [29]. Other studies have reported conventional machine learning methods based on manual features or two-dimensional (2D) CNN models to detect intracranial aneurysms from MRA images [8–12]. Miki et al. [8] and Stepan-Buksakowska et al. [9] used computer-aided diagnosis tools to detect intracranial aneurysms from MRA images, with average sensitivities of 82% and 83.6%, respectively. Another study applied a 2D CNN model to diagnose intracranial aneurysms in 2D maximum intensity projections (MIPs) of MRI and achieved a sensitivity of 94.2% [12]. However, the work was limited to the 2D projection of MRIs.

Our study revealed that the size of intracranial aneurysms can affect the performance of the 3D CNN system for intracranial aneurysm detection. For small intracranial aneurysms (< 3 mm), the 3D CNN system exhibited a sensitivity of 66.7%, which was higher than that previously reported for detecting intracranial aneurysms of similar size from CTA images [19]. For large and medium intracranial aneurysms, our system exhibited extremely high sensitivity (100%). Compared with the previous results of Sichtermann et al., the sensitivity of the 3D CNN system in detecting medium- and small-sized intracranial aneurysms from CTA images was higher than that from 3DTOF-MRA images. Among the four different models tested by Sichtermann et al., the maximum sensitivities were 38, 96, and 100% for small, medium, and large intracranial aneurysms, respectively. In our study, only four of the 98 intracranial aneurysms in the training dataset were small (< 3 mm) and the sensitivity of detecting these aneurysms using this training dataset was 66.7%. These findings suggest that the next step should be to label a group of subjects with small intracranial aneurysms in the training dataset. With an increase in samples with small intracranial aneurysms in the training dataset, the detection sensitivity of small intracranial aneurysms is expected to be further improved.

The overall sensitivity of our established 3D CNN system to segment intracranial aneurysms from CTA images was 92.3%. To further investigate the performance of the proposed system in the automatic segmentation of intracranial aneurysms from CTA images, the segmentation results generated by the 3D CNN system and those manually labeled by a well-trained radiologist were compared. In terms of preserving the original shape of intracranial aneurysms, 33.3% of the segmentation was better, 16.7% was consistent, and 50% was worse in the segmentation performed using the 3D CNN system, as compared with the segmentation results of the radiologist. Additionally, the segmentation performance of the proposed system was closely related to the size of intracranial aneurysms. In general, except in one particular case, the segmentation results for large- and medium-sized intracranial aneurysms were better than those for small aneurysms. In the outlying case, the segmentation result for a large intracranial aneurysm with a diameter of 24 mm was significantly worse than that of manual labeling by the radiologist, which may be associated with the evident low-density thrombus around the intracranial aneurysm. The specific reasons for this outcome need to be further explored. Moreover, the confidence values of the intracranial aneurysms segmented using the 3D CNN system were reliable. In the segmentation results generated by the 3D CNN system using the test dataset, 50% had a probability of 0.9999 or 1, 33.3% had a probability of ≥ 0.95, and the remaining 16.7% had a probability of ≥ 0.85.

In addition, the false-positive findings on the probability maps of the 3D CNN segmentation outputs were analyzed. More than 99% of the false-positive findings were located in very small clusters with very few voxels (less than five, where true intracranial aneurysm clusters usually consist of > 150 voxels), and more than 95% of those clusters had a probability of less than 0.8. Therefore, false positives can be significantly reduced by setting the cluster range threshold to > 5 and the probability threshold to > 0.8. The remaining clusters with a probability > 0.8 were non-aneurysm vascular regions with changes in vascular lumen diameter, such as slight widening of the local cerebral artery, slight depression of one artery wall, dilated artery after stenosis, or widening tentorial foot of the cerebellum. The presence of false positives in areas of non-aneurysm vessels with varying diameters may be clinically significant because radiologists should describe or report these areas in clinical practice.

This study had some limitations. First, our conclusions need to be further validated using larger sample numbers in the test and training datasets. Additionally, patients with intracranial aneurysms were included in both the training and test datasets. However, in clinical practice, the prevalence of intracranial aneurysms in the general population is relatively low. Therefore, datasets containing patients without intracranial aneurysms should be used for validation.

Conclusions

In conclusion, our established 3D CNN system implemented using the DeepMedic platform can reliably detect and segment intracranial aneurysms from CTA images. The size of intracranial aneurysms significantly influenced the performance of this segmentation system. The detection sensitivity for large and medium intracranial aneurysms was extremely high (100%), whereas the sensitivity for small intracranial aneurysms was lower (66.7%) but still higher than that reported in previous studies. Our work revealed that our established 3D CNN segmentation system has a high sensitivity in the segmentation of intracranial aneurysms and promising potential to yield an auto-segmented shape of intracranial aneurysms of even greater accuracy than the shape obtained from manual segmentations performed by radiologists. This lays the foundation for the clinical diagnostic application of the 3D CNN system implemented using the DeepMedic platform.

Supplementary Information The online version contains supplementary material available at https://doi.org/10.1007/s10278-022-00698-5.

Author Contribution XL and JM: literature search, study design, data collection, data processing and experimentation, data analysis and interpretation, and manuscript writing; NS and LC: data processing and experimentation; XY, YT, JW, and JL: data collection and manual labeling of CTA images of People's Hospital (Zhuhai Hospital Affiliated with Jinan University); HT and KW: data collection of DSA and surgery; LY, JL, YW, and BZ: data analysis and interpretation; YW and MC: data collection and manual labeling of CTA images of the First Affiliated Hospital of Harbin Medical University; and ZW and LL: study design, data analysis and interpretation, and manuscript writing.

Funding This study was supported in part by the National Natural Science Foundation of China (81601558), Breeding Foundation of Zhuhai People's Hospital of China (2019PY-16), and the Medical Research Foundation of Zhuhai City of China (20191207A010017).

Availability of Data and Materials Data used to support the findings of this study are available from the corresponding author upon request.

Code Availability Not applicable.

Declarations

Ethics Approval This retrospective study was approved by the Ethics Committee of Zhuhai People's Hospital and the First Affiliated Hospital of Harbin Medical University. Informed consent was obtained from all participants.

Consent to Participate Verbal informed consent was obtained prior to the interview.

Consent for Publication Participants have consented to the submission of the case report to the journal.

Conflict of Interest The authors declare no competing interests.

References

1. Etminan N, Dorfler A, Steinmetz H: Unruptured Intracranial Aneurysms- Pathogenesis and Individualized Management. Dtsch Arztebl Int 117:235-242, 2020
2. Laarman MD, et al.: Intracranial Aneurysm-Associated Single-Nucleotide Polymorphisms Alter Regulatory DNA in the Human Circle of Willis. Stroke 49:447-453, 2018
3. Suarez JI, Tarr RW, Selman WR: Aneurysmal subarachnoid hemorrhage. N Engl J Med 354:387-396, 2006
4. Rinkel GJ: Natural history, epidemiology and screening of unruptured intracranial aneurysms. Rev Neurol (Paris) 164:781-786, 2008
5. Pedersen HK, et al.: CTA in patients with acute subarachnoid haemorrhage. A comparative study with selective, digital angiography and blinded, independent review. Acta Radiol 42:43–49, 2001
6. Duan H, Huang Y, Liu L, Dai H, Zhou LJBEO: Automatic detection on intracranial aneurysm from digital subtraction angiography with cascade convolutional neural networks18, 2019
7. Chen X, et al.: Meta-analysis of computed tomography angiography versus magnetic resonance angiography for intracranial aneurysm97, 2018
8. Miki, et al.: Computer-Assisted Detection of Cerebral Aneurysms in MR Angiography in a Routine Image-Reading Environment: Effects on Diagnosis by Radiologists, 2016
9. Stepan-Buksakowska IL, et al.: Computer-aided diagnosis improves detection of small intracranial aneurysms on MRA in a clinical setting. AJNR Am J Neuroradiol 35:1897-1902, 2014
10. Yang X, Blezek DJ, Cheng LTE, Ryan WJ, Kallmes DF, Erickson BJJJoDI: Computer-aided detection of intracranial aneurysms in MR angiography24:86–95, 2011

11. Faron A, et al.: Performance of a Deep-Learning Neural Network to Detect Intracranial Aneurysms from 3D TOF-MRA Compared to Human Readers, 2019
12. Nakao T, et al.: Deep neural network-based computer-assisted detection of cerebral aneurysms in MR angiography, 2018
13. Lecun Y, Bengio Y, Hinton GJN: Deep learning521:436, 2015
14. Suzuki, Physics KJR, Technology: Overview of deep learning in medical imaging, 2017
15. Shen D, Wu G, Suk HIJARoBE: Deep Learning in Medical Image Analysis19:221-248, 2017
16. Litjens G, et al.: A Survey on Deep Learning in Medical Image Analysis42:60-88, 2017
17. Dai X, et al.: Deep learning for automated cerebral aneurysm detection on computed tomography images. Int J Comput Assist Radiol Surg 15:715-723, 2020
18. Park A, et al.: Deep Learning-Assisted Diagnosis of Cerebral Aneurysms Using the HeadXNet Model. JAMA Netw Open 2:e195600, 2019
19. Shi Z, et al.: A clinically applicable deep-learning model for detecting intracranial aneurysm in computed tomography angiography images. Nat Commun 11:6090, 2020
20. Kamnitsas K, et al.: Efficient Multi-Scale 3D CNN with Fully Connected CRF for Accurate Brain Lesion Segmentation36:61, 2016
21. Ren S, He K, Girshick R, Sun JJIToPA, Intelligence M: Faster R-CNN: Towards Real-Time Object Detection with Region Proposal Networks39:1137-1149, 2017
22. Szegedy C, et al.: Going Deeper with Convolutions, 2014
23. Redmon J, Divvala S, Girshick R, Farhadi A: You Only Look Once: Unified, Real-Time Object Detection. Proc. Computer Vision & Pattern Recognition: City
24. Redmon J, Farhadi AJae-p: YOLOv3: An Incremental Improvement, 2018
25. Albarqouni S, Baur C, Achilles F, Belagiannis V, Demirci S, Navab NJIToMI: AggNet: Deep Learning From Crowds for Mitosis Detection in Breast Cancer Histology Images35:1313-1321, 2016
26. Hirasawa T, Aoyama K, Tanimoto T, Ishihara S, Tada TJGCO-JotIGCA, Association tJGC: Application of artificial intelligence using a convolutional neural network for detecting gastric cancer in endoscopic images87:1–8, 2018
27. Setio AAA, et al.: Pulmonary Nodule Detection in CT Images: False Positive Reduction Using Multi-View Convolutional Networks35:1160-1169, 2016
28. Öman O, Mäkelä T, Salli E, Savolainen S, Kangasniemi MJERE: 3D convolutional neural networks applied to CT angiography in the detection of acute ischemic stroke3, 2019
29. Sichtermann T, Faron A, Sijben R, Teichert N, Freiherr J, Wiesmann MJAJoN: Deep learning-based detection of intracranial aneurysms in 3D TOF-MRA, 2018